

See discussions, stats, and author profiles for this publication at: <https://www.researchgate.net/publication/231679328>

# Formation Process of Ultrathin Multilayer Films of Molybdenum Oxide by Alternate Adsorption of Octamolybdate and Linear Polycations

ARTICLE *in* LANGMUIR · JANUARY 1998

Impact Factor: 4.46 · DOI: 10.1021/la970797g

---

CITATIONS

131

---

READS

6

5 AUTHORS, INCLUDING:



Yuri M Lvov

Louisiana Tech University

289 PUBLICATIONS 13,648 CITATIONS

SEE PROFILE



Toyoki Kunitake

FAIS

670 PUBLICATIONS 20,413 CITATIONS

SEE PROFILE

# Formation Process of Ultrathin Multilayer Films of Molybdenum Oxide by Alternate Adsorption of Octamolybdate and Linear Polycations

Izumi Ichinose,<sup>†</sup> Hideo Tagawa,<sup>†</sup> Suguru Mizuki,<sup>†</sup> Yuri Lvov,<sup>‡</sup> and Toyoki Kunitake<sup>\*,†</sup>

Department of Chemical Science & Technology, Faculty of Engineering, Kyushu University, Fukuoka 812, Japan, and Supermolecules Project, JST, Kurume Research Center, Kurume 839, Japan

Received July 16, 1997. In Final Form: October 20, 1997<sup>®</sup>

Multilayer films of molybdenum oxide were prepared by means of alternate adsorption of ammonium octamolybdate ((NH<sub>4</sub>)<sub>4</sub>[Mo<sub>8</sub>O<sub>26</sub>]) and poly(allylamine hydrochloride) (PAH). The films were reproducibly grown at each adsorption cycle, as monitored by a quartz crystal microbalance. Adsorption of PAH on the surface of a molybdenum oxide layer was saturated with a constant thickness of 32 ± 21 Å. On the other hand, adsorption of octamolybdate on the PAH layer did not show saturation. The thickness of the oxide layer in the individual adsorption step increased with the adsorption time at a rate of ca. 5.7 Å/min due to condensation of the adsorbed octamolybdate and the resulting loss of negative charges. The surface of the resulted films was relatively flat with height difference of less than 10 nm, and the film thickness was constant over a large area, as confirmed by scanning electron microscopy.

## 1. Introduction

Fabrication of inorganic thin films via stepwise adsorption has been widely studied for the purpose of surface modification and for the construction of functional materials.<sup>1</sup> In his pioneering work, Iler reported alternate adsorption of negatively charged silica colloids and positively charged alumina fibrils using electrostatic interaction.<sup>2</sup> Photochemically or electrochemically functionalized thin films have been prepared by taking advantage of stepwise coordination of diphosphoric compounds and zirconium ion.<sup>3</sup> Thickness control of metal oxide thin films was achieved by buildup of oxide thin films formed at the air–water interface<sup>4</sup> or by stepwise adsorption of metal alkoxides or trichlorosilane derivatives on hydrolyzed surfaces.<sup>5</sup> Alternate adsorption of oppositely charged polymers, as developed by Decher et al.,<sup>6</sup> has been extended to many inorganic polymers. Charged two-dimensional inorganic materials such as clay<sup>7</sup> and zirconium phosphates<sup>8</sup> and nanosized particles composed

of metal,<sup>9</sup> semiconductor,<sup>10</sup> or silica<sup>11</sup> have been used for the alternate adsorption in combination with oppositely charged organic polymers.

Polyoxometalates with well-defined primary structures are recently attracting much attention as building units of novel inorganic materials that are useful in catalysis, solid state devices, photo- and electrochromic display, biochemistry, and medicine.<sup>12</sup> Mallouk et al. reported that [Al<sub>13</sub>O<sub>4</sub>(OH)<sub>24</sub>(H<sub>2</sub>O)<sub>12</sub>]<sup>7+</sup> ions can be alternately adsorbed with zirconium phosphate (α-Zr(HPO<sub>4</sub>)<sub>2</sub>) that is exfoliated to single, separate layers.<sup>8</sup> In this case, ellipsometric measurements show uniform film growth with thickness increase of 16 Å at each adsorption cycle. Ingersoll, Kulesza, and Faulkner carried out alternate adsorption of polyoxometalates (isopolymolybdate, phosphotungstate, or silicotungstate) with cationic polymers on carbon electrode and confirmed their systematic growth by cyclic voltammetry.<sup>13</sup>

We have been conducting detailed examination of alternate adsorption steps of a large variety of organic, inorganic, and biological materials.<sup>14</sup> The film growth in the individual adsorption step can be quantitatively monitored by a quartz crystal microbalance (QCM). During the course of these investigations, we found that the adsorption process of ammonium octamolybdate showed unique time-dependent characteristics. In this paper, we describe a detailed study of the formation of the

<sup>†</sup> Kyushu University.

<sup>‡</sup> Supermolecules Project.

<sup>®</sup> Abstract published in *Advance ACS Abstracts*, December 15, 1997.

(1) (a) Fendler, J. H.; Meldrum, F. C. *Adv. Mater.* **1995**, *7*, 607. (b) Mallouk, T. E.; Kim, H.-N.; Ollivier, P. J.; Keller, S. W. In *Comprehensive Supramolecular Chemistry*; Alberti, G., Ed.; Elsevier Science: Amsterdam, 1996; pp 189–218. (c) Yitzchaik, S.; Marks, T. J. *Acc. Chem. Res.* **1996**, *29*, 197.

(2) Iler, R. K. *J. Colloid Interface Sci.* **1966**, *21*, 569.

(3) (a) Cao, G.; Hong, H.-G.; Mallouk, T. E. *Acc. Chem. Res.* **1992**, *25*, 420. (b) Bell, C. M.; Arendt, M. F.; Gomez, L.; Schmehl, R. H.; Mallouk, T. E. *J. Am. Chem. Soc.* **1994**, *116*, 8374.

(4) (a) Moriguchi, I.; Maeda, H.; Teraoka, Y.; Kagawa, S. *J. Am. Chem. Soc.* **1995**, *117*, 1139. (b) Mirley, C. L.; Koberstein, J. T. *Langmuir* **1995**, *11*, 1049.

(5) (a) Ichinose, I.; Senzu, H.; Kunitake, T. *Chem. Lett.* **1996**, 831.

(b) Brunner, H.; Vallant, T.; Mayer, U.; Hoffmann, H. *Langmuir* **1996**, *12*, 4614.

(6) Decher, G.; Hong, J. D. *Ber. Bunsenges. Phys. Chem.* **1991**, *95*, 1430.

(7) (a) Kleinfeld, E. R.; Ferguson, G. S. *Science* **1994**, *265*, 370. (b) Ferguson, G. S.; Kleinfeld, E. R. *Adv. Mater.* **1995**, *7*, 414. (c) Lvov, Y.; Ariga, K.; Ichinose, I.; Kunitake, T. *Langmuir* **1996**, *12*, 3038.

(8) Keller, S. W.; Kim, H.-N.; Mallouk, T. E. *J. Am. Chem. Soc.* **1994**, *116*, 8817.

(9) Schmitt, J.; Decher, G. *Adv. Mater.* **1997**, *9*, 61.

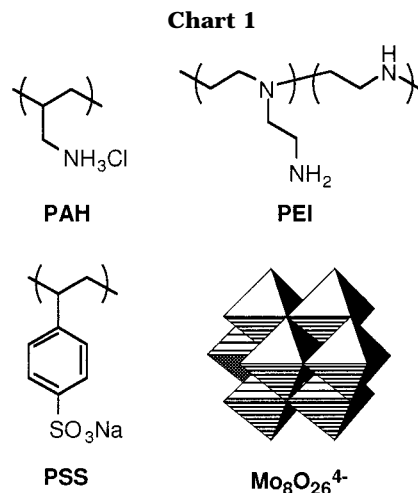
(10) (a) Gao, M.; Gao, M.; Zhang, X.; Yang, Y.; Yang, B.; Shen, J. *J. Chem. Soc., Chem. Commun.* **1994**, 2777. (b) Kotov, N. A.; Dekany, I.; Fendler, J. H. *J. Phys. Chem.* **1995**, *99*, 13065.

(11) (a) Krozer, A.; Nordin, S.-A.; Kasemo, B. *J. Colloid Interface Sci.* **1995**, *176*, 479. (b) Ariga, K.; Lvov, Y.; Onda, M.; Ichinose, I.; Kunitake, T. *Chem. Lett.* **1997**, 125.

(12) Pope, M. T.; Muller, A. *Angew. Chem., Int. Ed. Engl.* **1991**, *30*, 34.

(13) Ingersoll, D.; Kulesza, P. J.; Faulkner, L. R. *J. Electrochem. Soc.* **1994**, *141*, 140.

(14) Sano, M.; Lvov, Y.; Kunitake, T. *Annu. Rev. Mater. Sci.* **1996**, *26*, 153.



molybdenum oxide layer by alternate adsorption of octamolybdate anion and linear polycations.

## 2. Experimental Section

**Materials.** Ammonium octamolybdate,  $(\text{NH}_4)_4[\text{Mo}_8\text{O}_{26}] \cdot 5\text{H}_2\text{O}$  (MW 1345.8), was prepared according to the method of Aveston et al.<sup>15</sup> Briefly, aqueous sodium molybdate ( $\text{Na}_2\text{MoO}_4 \cdot 2\text{H}_2\text{O}$ , 14.5 g) was applied to a cation exchange column (Dowex 50w  $\times$  8; H-form; 5.2 mequiv/g, ca. 100 g), and the elute was directly poured into aqueous ammonium paramolybdate,  $(\text{NH}_4)_6[\text{Mo}_7\text{O}_{24}] \cdot 4\text{H}_2\text{O}$  (Kishida Chem., 14.8 g), with stirring. The mixture (ca. 2000 mL) was concentrated to ca. 50 mL by blowing air. Colorless cubic crystals were collected on a suction filter, washed with a small amount of deionized water, and air-dried with a yield of 18.5 g. IR (KBr) 941.4, 906.7, 852.6, 719.5, 555.6, 520.8  $\text{cm}^{-1}$ .<sup>16</sup>

Poly(allylamine hydrochloride) (PAH; MW 50,000; Aldrich), sodium poly(styrenesulfonate) (PSS; MW 100,000; Am. Polym. Standard), and poly(ethylenimine) (PEI; MW 70,000; Sci. Polym. Products) were used as purchased without further purification. The polymer solutions used were 0.9 mg/mL, pH 2.5–3.0, for PAH, 3.0 mg/mL, pH 4.0, for PSS, and 1.5 mg/mL, pH 9.0, for PEI. The pH was adjusted by adding aqueous HCl.  $(\text{NH}_4)_4[\text{Mo}_8\text{O}_{26}]$  was used immediately after preparation at a concentration of 10 mg/mL (pH 3.5). Structures of  $[\text{Mo}_8\text{O}_{26}]^{4-}$  ion<sup>17</sup> and polymers used are shown in Chart 1.

**Quartz Crystal Microbalance.** A quartz crystal microbalance (QCM) device manufactured by USI System, Fukuoka, was used for monitoring the  $(\text{NH}_4)_4[\text{Mo}_8\text{O}_{26}]/\text{PAH}$  assembly. The resonator was covered by evaporated silver electrodes with a surface area of 0.159  $\text{cm}^2$ , and the resonance frequency was 9 MHz. Before each QCM experiment, the resonator was washed in 1 wt % KOH solution ( $\text{EtOH}:\text{H}_2\text{O} = 3:2$ ) for 80 s at 50  $^\circ\text{C}$  under weak sonication, rinsed with pure water for 1 min, and dried with nitrogen gas. It was then immersed in PEI solution at pH 9.0 for 15 min, rinsed with pure water, and dried with nitrogen gas. The positively charged surface was further immersed in PSS solution at pH 4.0 and in PEI solution at pH 9.0.<sup>18</sup> The electrode with a PEI/PSS/PEI precursor film was then alternately immersed in aqueous  $(\text{NH}_4)_4[\text{Mo}_8\text{O}_{26}]$  for 4–35 min and in PAH solution for 20 min with intermediate water washing and drying. Frequency of QCM was monitored in each adsorption step after drying.

We estimated a mass increase due to film growth from frequency shifts of QCM by using the Sauerbrey equation.<sup>19</sup> A frequency decrease of 1 Hz corresponds to a mass increase of 0.9

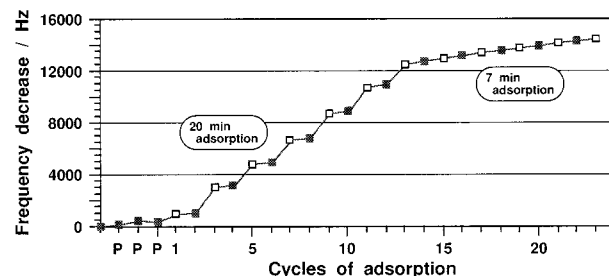


**Figure 1.** QCM frequency shift ( $-\Delta F$ ) of alternate adsorption of  $(\text{NH}_4)_4[\text{Mo}_8\text{O}_{26}]$  and PAH on a PEI/PSS/PEI precursor film. The first three plots denoted as P are adsorption of the precursor layer: ( $\square$ )  $(\text{NH}_4)_4[\text{Mo}_8\text{O}_{26}]$  adsorption; ( $\blacksquare$ ) PAH adsorption. An aqueous  $(\text{NH}_4)_4[\text{Mo}_8\text{O}_{26}]$  of 10 mg/mL, pH 3.5, was used for all the adsorptions at 25  $^\circ\text{C}$ . The period of adsorption of PAH (0.9 mg/mL, pH 2.5–3.0) was 20 min.

ng in our system. Thickness ( $d$ ) of an adsorbed film on one side of the electrode is given as follows

$$2d(\text{\AA}) = -\Delta F(\text{Hz})/1.832\rho(\text{g/cm}^3) \quad (1)$$

where  $\rho$  is the density of adsorbed film and  $\Delta F$  is the frequency shift of QCM. We used here bulk densities of 1.2 and 3.06  $\text{g/cm}^3$  for PAH<sup>18</sup> and molybdenum oxide,<sup>20</sup> respectively. Validity of the use of these bulk density values was confirmed by comparing film thickness (scanning electron microscopy) and film mass (QCM) as described below. The kinetic process of alternate adsorption was followed by using an *in situ* QCM technique elaborated by Ebara and Okahata<sup>21</sup> and Lvov et al.<sup>18</sup>

**Other Measurements.** Scanning electron micrographs were obtained with a Hitachi S-900 instrument at an acceleration voltage of 25 kV. The samples were coated with 20  $\text{\AA}$  thick Pt by use of an ion coater (Hitachi E-1030 ion sputter, 10 mA/10 Pa) under argon atmosphere to prevent the charge up. Fourier transform infrared (FT-IR) reflection spectra and UV absorption spectra were obtained by using a Nicolet 710 FT-IR spectrometer and a JASCO V-570 spectrophotometer, respectively.<sup>22</sup> X-ray photoelectron spectra (XPS) were obtained with a Perkin-Elmer PHI 5300 ESCA system at a take-off angle of 45 $^\circ$ .<sup>22</sup> The charging shift was corrected by the binding energy of carbon.

## 3. Results and Discussion

**Adsorption Process.** Poly(ethylenimine) (PEI) and poly(styrenesulfonate) (PSS) were alternately adsorbed on a silver-coated QCM resonator in order to prepare a PEI/PSS/PEI precursor film.<sup>18</sup> The precursor film is essential for forming smooth and uniformly charged surfaces on the QCM electrode and for the subsequent reproducible adsorption. Alternate assembly of  $(\text{NH}_4)_4[\text{Mo}_8\text{O}_{26}]$  and PAH is remarkably dependent on the pH value of the PAH solution. Preliminary experiments revealed that alternate adsorption did not proceed with a PAH solution of pH 5–6 and that the molybdenum oxide layer occasionally dissolved in aqueous PAH of pH 4. On the other hand, it was difficult to avoid corrosion of the QCM electrode under acidic conditions below pH 2.0. Therefore, the pH of the PAH solution was adjusted to 2.5–3.0 by adding aqueous HCl.  $(\text{NH}_4)_4[\text{Mo}_8\text{O}_{26}]$  was used simply by dissolving in pure water at a concentration of 10 mg/mL (pH 3.5).<sup>23</sup>

Figure 1 shows a frequency decrement ( $-\Delta F$ ) of QCM

(15) Aveston, J.; Anacker, E. W.; Johnson, J. S. *Inorg. Chem.* **1964**, 3, 735.

(16) (a) Klemperer, W. G.; Shum, W. J. *Am. Chem. Soc.* **1976**, 98, 8291. (b) Coddington, J. M.; Taylor, M. J. *J. Chem. Soc., Dalton Trans.* **1990**, 41.

(17) Wells, A. F. *Structural Inorganic Chemistry*; Clarendon Press: Oxford, 1984.

(18) Lvov, Y.; Ariga, K.; Ichinose, I.; Kunitake, T. *J. Am. Chem. Soc.* **1995**, 117, 6117.

(19) Sauerbrey, G. *Z. Phys.* **1959**, 155, 206.

(20) Weakley, T. J. R. *Polyhedron* **1982**, 1, 17.

(21) Ebara, Y.; Okahata, Y. *J. Am. Chem. Soc.* **1994**, 116, 11209.

(22) Ikeura, Y.; Kurihara, K.; Kunitake, T. *J. Am. Chem. Soc.* **1991**, 113, 7342.

(23) In the case a silver-coated QCM electrode without precursor film immersed in aqueous  $(\text{NH}_4)_4[\text{Mo}_8\text{O}_{26}]$  (10 mg/mL, pH 3.5) for 14 h, the frequency decrease was 143 Hz. This shift is very small as compared with the total frequency shifts in our alternate adsorption experiments.

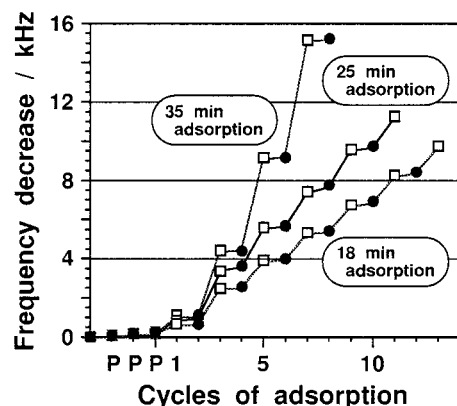


**Figure 2.** Dependence of QCM frequency shift on the period of adsorption: (□)  $(\text{NH}_4)_4[\text{Mo}_8\text{O}_{26}]$  adsorption; (●) PAH adsorption. The period of adsorption of  $(\text{NH}_4)_4[\text{Mo}_8\text{O}_{26}]$  is varied for the three series of experiments as indicated. PAH was adsorbed for 15 min for all the experiments.

resonator during alternate adsorption of  $(\text{NH}_4)_4[\text{Mo}_8\text{O}_{26}]$  and PAH. The resonator was immersed in  $(\text{NH}_4)_4[\text{Mo}_8\text{O}_{26}]$  solution for 20 min up to the 13th cycle and for 7 min from the 14th cycle on. Immersion time in PAH solution was 20 min in all the adsorption cycles. One adsorption cycle consists of three steps: adsorption of  $(\text{NH}_4)_4[\text{Mo}_8\text{O}_{26}]$  or PAH, rinsing with pure water, and drying. The adsorptions were reproducible except for the first adsorption on the precursor film. This indicates that molybdenum oxide and PAH layers grow regularly on the electrode. Adsorption of PAH on the molybdenum oxide layer is uniform for all the cycles, as shown in Figure 1, with a frequency change of  $156 \pm 90$  Hz. On the other hand, adsorption of  $(\text{NH}_4)_4[\text{Mo}_8\text{O}_{26}]$  on the PAH layer is evidently affected by the immersion time. The frequency change is  $1775 \pm 261$  Hz for the 20-min adsorption and  $224 \pm 27$  Hz for the 7-min adsorption. This dependence was also confirmed by the measurement of the adsorption kinetics using the *in situ* QCM technique, in which adsorption of PAH on the molybdenum oxide layer was saturated within 10 min but that of  $(\text{NH}_4)_4[\text{Mo}_8\text{O}_{26}]$  on the PAH layer proceeded without saturation.

In general, adsorption of oppositely charged polymers becomes saturated when the surface charge is reversed by overcompensation. However, such saturation is not observed for the adsorption of  $(\text{NH}_4)_4[\text{Mo}_8\text{O}_{26}]$ . The molybdenum oxide layers prepared at different adsorption times must produce similarly-charged, negative surfaces in spite of varying extents of adsorption, because adsorption of PAH is constant with a frequency shift of ca. 150 Hz. The lack of saturation may be explained by loss of the negative charge on the molybdenum oxide layer during the course of adsorption. Aqueous solutions of  $(\text{NH}_4)_4[\text{Mo}_8\text{O}_{26}]$  are known to contain not only  $[\text{Mo}_8\text{O}_{26}]^{4-}$  ions but also its protonated and condensed species.<sup>24</sup> If the adsorbed species such as  $\text{H}_n[\text{Mo}_8\text{O}_{26}]^{n-4}$  and  $[\text{Mo}_8\text{O}_{25}]^{2n-}$  ions are further protonated and condensed at the negatively-charged surface of molybdenum oxide layer, the resulting loss of the negative charge should be able to induce further adsorption of octamolybdates. Then, the adsorption of  $(\text{NH}_4)_4[\text{Mo}_8\text{O}_{26}]$  may not reach saturation. Co-adsorption of  $\text{NH}_4^+$  ion suggested by the XPS data will also contribute to neutralization of the surface negative charge.

Frequency changes of molybdenum oxide/PAH assembly at different immersion times are shown in Figure 2.

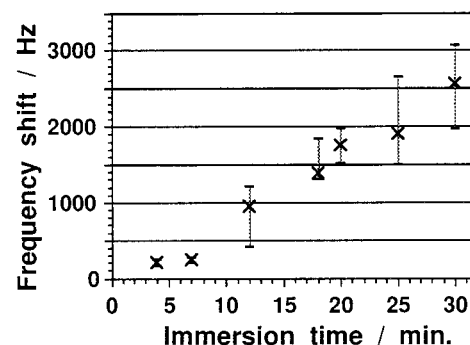


**Figure 3.** Variation of QCM frequency shifts in the  $(\text{NH}_4)_4[\text{Mo}_8\text{O}_{26}]$  adsorption: (x) average frequency shifts of four to six repeated adsorptions within one series of experiments. Data obtained for adsorption periods of 4, 7, 12, 18, 20, 25, and 30 min are shown. The periods of adsorption of PAH are 15 or 20 min, giving a constant frequency shift of ca. 150 Hz.

$(\text{NH}_4)_4[\text{Mo}_8\text{O}_{26}]$  was reproducibly adsorbed at 18-min and 25-min adsorption with frequency shifts of  $1403 \pm 443$  and  $1916 \pm 734$  Hz, respectively. The corresponding frequency changes for PAH adsorption were  $132 \pm 72$  and  $173 \pm 132$  Hz, respectively. At the 35-min adsorption, however, the frequency shift due to  $(\text{NH}_4)_4[\text{Mo}_8\text{O}_{26}]$  adsorption gradually increased from 3331 to 5946 Hz with repeated adsorption cycles, and the amount of PAH adsorbed was diminished to about one-third of the above two cases ( $57 \pm 28$  Hz). Fresh  $(\text{NH}_4)_4[\text{Mo}_8\text{O}_{26}]$  solutions were individually prepared for each experiment in Figure 2. And the period of the total immersion experiment in the case of the 35-min adsorption was 140 min (35 min  $\times$  4) for the total four cycles. This period is almost the same as that of 25-min adsorption (150 min for six cycles) and 18-min adsorption (126 min for seven cycles). Therefore, the increase in frequency shift in the individual 35-min adsorption is not caused by aging of the  $(\text{NH}_4)_4[\text{Mo}_8\text{O}_{26}]$  solutions used. Protonation and condensation of the molybdenum oxide species may be accelerated at the molybdenum oxide surface, if the contact time is sufficiently long (35-min adsorption). The decrease in corresponding adsorption of PAH is consistent with this presumption. Formation of the PAH layer at appropriate intervals is essential for the controlled growth of molybdenum oxide layers.

**Film Structure.** Figure 3 shows a relationship between the period of immersion in aqueous  $(\text{NH}_4)_4[\text{Mo}_8\text{O}_{26}]$  and the corresponding QCM frequency shift. The average values of the frequency shifts are marked with crosses in this figure. The frequency is proportional to the immersion period with a slope of 63 Hz/min. If we can assume that the density of ammonium octamolybdate ( $(\text{NH}_4)_4[\text{Mo}_8\text{O}_{26}] \cdot 5\text{H}_2\text{O}$ ,  $3.06 \text{ g/cm}^3$ )<sup>20</sup> is identical with that of the molybdenum oxide layer formed, this slope corresponds to a thickness increase of  $5.7 \text{ \AA/min}$  from eq 1. The size of  $[\text{Mo}_8\text{O}_{26}]^{4-}$  ion estimated by molecular mechanics calculation (MM2, SONY Tektronix CAChe System) is  $10.3 \times 7.3 \times 9.8 \text{ \AA}^3$ , and the density calculated from its size and molecular weight (MW: 1183.5) is  $2.67 \text{ g/cm}^3$ . When the  $[\text{Mo}_8\text{O}_{26}]^{4-}$  ion deposits on a QCM electrode in the closest packing, the layer thickness due to a frequency change of  $194 \pm 35$  Hz (for 4-min adsorption) is calculated as  $20 \pm 4 \text{ \AA}$  from eq 1, and corresponds to two to three layers of the  $[\text{Mo}_8\text{O}_{26}]^{4-}$  unit. The thickness increase for 30-min adsorption ( $2587 \pm 609$  Hz) is  $264 \pm 62 \text{ \AA}$ , corresponding to about 30 layers of the  $[\text{Mo}_8\text{O}_{26}]^{4-}$  unit. Similarly, the frequency shift of  $156 \pm 90$  Hz for PAH (Figure 1) corresponds to a thickness increase of  $32 \pm 21 \text{ \AA}$ , by assuming a density of  $1.2 \text{ g/cm}^3$ .<sup>18</sup>

(24) Kepert, D. L. *The Early Transition Metals*; Academic Press: London and New York, 1972.

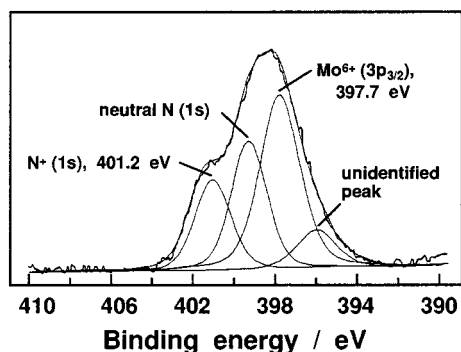


**Figure 4.** XPS spectrum of a molybdenum oxide/PAH multilayer. The sample was prepared on a gold-coated glass plate<sup>27</sup> with a PEI/PSS/PEI precursor film. The periods of adsorption are 30 min for  $(\text{NH}_4)_4[\text{Mo}_8\text{O}_{26}]$  (four cycles) and 20 min for PAH (three cycles). The outermost surface is molybdenum oxide layer.

The film growth of molybdenum oxide/PAH multilayers can be monitored on quartz plates by UV spectroscopy. The absorbance at 200–400 nm was linearly increased with the adsorption cycle. Since the spectra do not show absorption due to intervalence charge transfer transitions<sup>25</sup> at wavelengths beyond 500 nm, all molybdenum atoms in the multilayer film are  $\text{Mo}^{6+}$ . This is also confirmed by XPS measurement of the multilayer in the energy region of  $\text{Mo}_{3d}$ . The XPS spectrum gives only two peaks at 232.2 and 235.3 eV, attributable to  $\text{Mo}^{6+}(3d_{5/2})$  and  $\text{Mo}^{6+}(3d_{3/2})$ , respectively,<sup>26</sup> in agreement with the UV result. Degrees of protonation and/or condensation of polyoxomolybdate species in the multilayer may be estimated from the ratio of ammonium nitrogen and molybdenum atoms from XPS peak intensities, since the loss of negative charge due to protonation of  $[\text{Mo}_8\text{O}_{26}]^{4-}$  ion must be concurrent with the decrement of counter-cations from the original composition of  $\text{N}^+/\text{Mo} = 4:8$ . In the multilayer film, the counter-cations may be composed of  $\text{NH}_4^+$  ions and ammonium groups of PAH. Figure 4 shows the XPS spectrum of a molybdenum oxide/PAH multilayer in the energy region of  $\text{N}_{1s}$  and  $\text{Mo}_{3p}$ . Though an unidentified peak is included in the lower energy region, the spectrum can be deconvoluted to three Gaussian–Lorentz curves at binding energies of 401.2, 399.3, and 397.7 eV, which have been attributed to  $\text{N}^+(1s)$ , neutral  $\text{N}(1s)$ , and  $\text{Mo}^{6+}(3p_{3/2})$ , respectively.<sup>26</sup> The ratio of ammonium nitrogen against molybdenum atom is  $\text{N}^+/\text{Mo} = 0.25 \pm 0.1$ , as calculated from the peak areas of  $\text{N}^+(1s)$  and  $\text{Mo}^{6+}(3d_{5/2})$  after correction of relative sensitivity factors.<sup>26</sup> The  $\text{N}^+/\text{Mo}$  ratio observed is only half of that predicted for  $(\text{NH}_4)_4[\text{Mo}_8\text{O}_{26}]$ . Therefore, the octamolybdate species existing in the multilayer are probably protonated with two protons to give a composition of  $(\text{NH}_4)_2^{2+} \cdot [\text{H}_2\text{Mo}_8\text{O}_{26}]^{2-}$ . A thin molybdenum oxide layer is then represented as  $(\text{PAH})^{2+} \cdot [\text{H}_2\text{Mo}_8\text{O}_{26}]^{2-}$ . In the case where these protonated species are condensed by dehydration



the composition should be represented as  $(\text{NH}_4)_2^{2+} \cdot [\text{Mo}_8\text{O}_{25}]^{2-}$ .

A molybdenum oxide/PAH multilayer prepared on a gold-coated glass plate<sup>27</sup> gave broad peaks near 945 and 893  $\text{cm}^{-1}$  in FT-IR reflection spectra. These two peaks

are assigned to symmetrical and asymmetrical stretching vibrations of a  $\text{Mo}=\text{O}$  bond and are also observed for  $(\text{NH}_4)_4[\text{Mo}_8\text{O}_{26}]$  at 941 and 907  $\text{cm}^{-1}$ , respectively.<sup>16</sup> On the other hand, the peaks of  $\text{Mo}-\text{O}-\text{Mo}$  stretching vibrations observed at 853 and 720  $\text{cm}^{-1}$  for  $(\text{NH}_4)_4[\text{Mo}_8\text{O}_{26}]$  were not detected for the multilayer, and new peaks were observed near 680  $\text{cm}^{-1}$  instead. The latter peaks are probably attributed to weakened  $\text{Mo}-\text{O}-\text{Mo}$  stretching vibrations. It is apparent from these results that  $[\text{Mo}_8\text{O}_{26}]^{4-}$  ion in the multilayer is not merely made of the precipitates of  $(\text{NH}_4)_4[\text{Mo}_8\text{O}_{26}]$ . A most plausible structure existing in the layer is polymerized octamolybdates, such as  $(\text{NH}_4)_{2n}^{2n+} \cdot [\text{Mo}_8\text{O}_{25}]_n^{2n-}$  formed via protonation and condensation of  $[\text{Mo}_8\text{O}_{26}]^{4-}$  ions. This structure is consistent with the XPS film composition ( $\text{N}^+/\text{Mo} = 0.25$ ) and with the broadened  $\text{Mo}=\text{O}$  vibration peak and weakened  $\text{Mo}-\text{O}-\text{Mo}$  vibration peaks in FT-IR spectra.

Figure 5 shows scanning electron microscopy (SEM) micrographs of a molybdenum oxide/PAH multilayer prepared on a silver-coated QCM resonator. The left photo (Figure 5a) is a surface view. We selected a SEM picture with deep clefts. The depth (ca. 200 nm) of these clefts is consistent with the total thickness of the multilayer film estimated by QCM measurement (see below), and the silver electrode of the QCM resonator can be seen at the bottom of the cleft. The cleft is probably formed by lateral contraction of the film due to drying under high vacuum in the SEM observation. Apart from these clefts, the surface is surprisingly smooth over a large area. Gentle undulation of the film surface represents the roughness of the QCM resonator, as previously reported.<sup>18</sup> The right photo (Figure 5b) is a cross-sectional view. In this figure, the silver electrode is detached from quartz, and the multilayer film is located on the silver electrode with an almost identical thickness. The film has a constant thickness of  $210 \pm 10$  nm, and the surface roughness is estimated to be no more than 10 nm. Total frequency shift of the QCM measurement for the film shown in Figure 5 was 21 700 Hz. Film thickness calculated from the frequency shift and density of ammonium octamolybdate ( $3.06 \text{ g/cm}^3$ ) by using eq 1 is 194 nm. This thickness is slightly smaller than the SEM thickness of 210 nm. The agreement is satisfactory and the difference probably arises from an error in estimation of the film density, because the thickness calculation from QCM data is accurate with an experimental error of less than 10%.

**Adsorption Mechanism.** The alternate adsorption of  $(\text{NH}_4)_4[\text{Mo}_8\text{O}_{26}]$  and cationic polymers (PAH and PEI) is critically affected by pH of polymer solutions. This is typically shown by comparison of Figure 2 and Figure 6.  $(\text{NH}_4)_4[\text{Mo}_8\text{O}_{26}]$  is reproducibly adsorbed with PAH (pH 2.5–3.0), giving constant frequency shifts (Figure 2). In contrast, the adsorbed  $(\text{NH}_4)_4[\text{Mo}_8\text{O}_{26}]$  (10 mM, pH 3.5) layer is totally desorbed in the subsequent immersion in aqueous PEI at pH 9 (Figure 6). The frequency decrease due to adsorption of  $(\text{NH}_4)_4[\text{Mo}_8\text{O}_{26}]$  for 15 min is  $953 \pm 102$  Hz and the frequency increase during the subsequent step in aqueous PEI for 20 min is  $955 \pm 102$  Hz. Since at least 3% of the amino group in PEI is protonated at this pH,<sup>28</sup> the polymer can be readily adsorbed on negatively charged surfaces of QCM electrodes and glass plates, causing charge reversal to positive. However, the existing molybdenum oxide layer (ca. 10 nm thickness) is rather dissolved into the PEI solution. This desorption must be

(25) Buckley, R. I.; Clark, R. J. H. *Coord. Chem. Rev.* **1985**, *65*, 167.

(26) (a) Briggs, D.; Seah, M. P. *Practical Surface Analysis by Auger and X-ray Photoelectron Spectroscopy*; Wiley: New York, 1983. (b) *Handbook of X-ray Photoelectron Spectroscopy*; Perkin-Elmer: Eden Prairie, MN, 1978.

(27) A gold-coated glass plate was immersed in 3-mercaptopropionic acid solution (1 mM in ethanol) for 12 h, and used for the adsorption of PEI/PSS/PEI precursor film and the subsequent  $(\text{NH}_4)_4[\text{Mo}_8\text{O}_{26}]/\text{PAH}$  assembly.

(28) Suh, J.; Paik, H.-J.; Hwang, B. K. *Bioorg. Chem.* **1994**, *22*, 318.

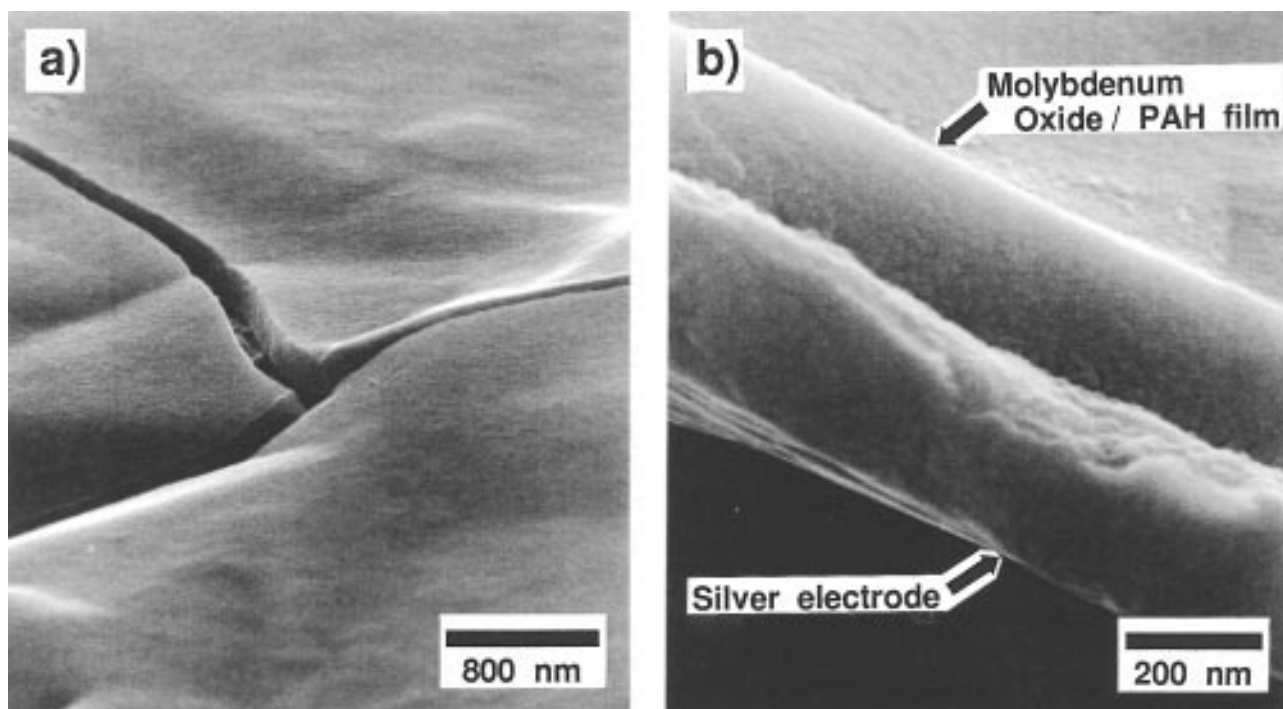


**Figure 5.** Scanning electron micrographs of a molybdenum oxide/PAH multilayer on a silver-coated QCM resonator: (a) surface view ( $\times 25000$ ), (b) cross-sectional view ( $\times 90000$ ). The sample was prepared at 35-min adsorption of  $(\text{NH}_4)_4[\text{Mo}_8\text{O}_{26}]$  (five cycles) and 20-min adsorption of PAH (five cycles) on a PEI/PSS/PEI precursor film. The total frequency shift is 21 700 Hz.

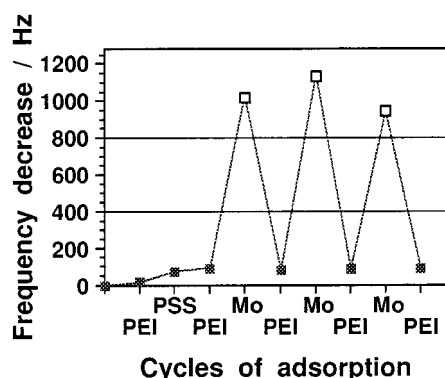


**Figure 6.** QCM frequency shift of alternate adsorption of  $(\text{NH}_4)_4[\text{Mo}_8\text{O}_{26}]$  and PEI. The period of adsorption is 20 min for a  $(\text{NH}_4)_4[\text{Mo}_8\text{O}_{26}]$  solution (10 mg/mL, pH 3.5) and 15 min for a PEI solution (1.5 mg/mL, pH 9.0), respectively.

caused by high solubility of the molybdenum oxide/PEI complex formed. We need to adjust pH of aqueous cationic polymers properly so as to prevent desorption of the molybdenum oxide layer.

Chemical structure of the cationic polymer may also affect adsorption of  $(\text{NH}_4)_4[\text{Mo}_8\text{O}_{26}]$ . As observed in all the experiments in Figure 1 and Figure 2, the amount of molybdenum oxide adsorbed on the precursor film with an outermost PEI layer is always smaller than that found in the subsequent adsorption on the PAH layer.

Alternate adsorption is not always feasible for small molecules and polymers. Aqueous bilayer membranes,<sup>29</sup> bolaform amphiphiles,<sup>30</sup> and several kinds of water-soluble dye molecules<sup>31</sup> can undergo alternate adsorption with

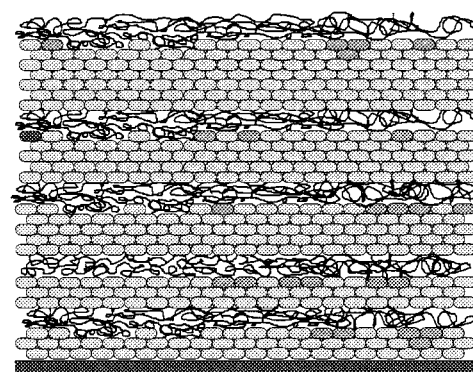


**Figure 7.** Schematic illustration of a molybdenum oxide/PAH multilayer. The first two oxide layers are composed of three layers of  $[\text{Mo}_8\text{O}_{26}]^{4-}$  units corresponding to the 4- and 7-min adsorptions of  $(\text{NH}_4)_4[\text{Mo}_8\text{O}_{26}]$ . PAH layers have a constant thickness of ca. 3 nm.

oppositely-charged polymers. In these cases, adsorbing species themselves form stable aggregates in water or at the surface. Aqueous  $(\text{NH}_4)_4[\text{Mo}_8\text{O}_{26}]$  (10 mM) forms precipitates, when it is allowed to stand at room temperature for a few months. For successful alternate adsorption, it is essential that a sufficiently insoluble layer of polyoxometalates is produced at the surface of cationic polymers. We separately observed repeated desorption such as shown in Figure 6 for  $[\text{V}_{10}\text{O}_{28}]^{6-}$  ion in alternate adsorption of PAH and  $[\text{V}_{10}\text{O}_{28}]^{6-}$  (10 mg/mL, in pure water). Similar desorption is observed in combination of PSS (pH 4.0, with HCl) and  $[\text{Cd}_{10}(\text{SCH}_2\text{CH}_2\text{OH})_{16}]^{4+}$  (10 mg/mL, in pure water). These metal clusters cannot form condensates or aggregates on the surface of oppositely-charged polymers.

It is surprising that molybdenum oxide/PAH multilayer films have uniform thicknesses with extremely smooth surfaces, in spite of the fact that the oxide layer grows via consecutive precipitation of polyoxomolybdates. Simple condensation of molybdenum oxide does not afford con-

(29) Ichinose, I.; Fujiyoshi, K.; Mizuki, S.; Lvov, Y.; Kunitake, T. *Chem. Lett.* **1996**, 257.

(30) (a) Decher, G.; Hong, J. D. *Makromol. Chem. Macromol. Symp.* **1991**, 46, 321. (b) Mao, G.; Tsao, Y.; Tirrell, N.; Davis, H. T.; Hessel, V.; Ringsdorf, H. *Langmuir* **1993**, 9, 3461.

(31) Ariga, K.; Lvov, Y.; Kunitake, T. *J. Am. Chem. Soc.* **1997**, 119, 2224.

tinuous growth of layers, since the linear film growth is not observed in the case of a long immersion in  $(\text{NH}_4)_4^-[\text{Mo}_8\text{O}_{26}]$  solution (Figure 2). The co-adsorption of PAH is essential. The adsorption of  $(\text{NH}_4)_4[\text{Mo}_8\text{O}_{26}]$  on PAH surface must be caused via electrostatic interaction. This type of adsorption becomes saturated when the surface charge is reversed. However, the polyoxomolybdates adsorbed on the PAH layer are capable of protonation and condensation, and the resulting loss of the negative charge is compensated by further adsorption of octamolybdates.

The multilayer films have PAH layers with a constant thickness of ca. 3 nm, and the thickness of the oxide layer can be controlled in a range of 2–25 nm by selection of

immersion period. Such a multilayer may be shown schematically as given in Figure 7. As shown in Figure 3, the thickness of the molybdenum oxide layer is constant for 4- and 7-min adsorptions of  $(\text{NH}_4)_4[\text{Mo}_8\text{O}_{26}]$ . The electrostatic interaction is a dominant factor for these adsorptions. This is contrasted to thickness increases at immersion periods longer than 12 min. The surface of the multilayer films is extremely smooth without regard to the thickness of the molybdenum oxide layer. Partial desorption of the molybdenum oxide layer and/or structural rearrangements of the adsorbed species during the succeeding PAH adsorption may produce smooth surfaces.

LA970797G